HHS Public Access

Author manuscript

J Immunol. Author manuscript; available in PMC 2019 May 01.

Published in final edited form as:

J Immunol. 2018 May 01; 200(9): 3218–3230. doi:10.4049/jimmunol.1701571.

Interferon regulatory factor 2 inhibits expression of glycolytic genes and lipopolysaccharide induced pro-inflammatory responses in macrophages

Huachun Cui[1], **Sami Banerjee**[1], **Sijia Guo**[1,2], **Na Xie**[1], and **Gang Liu**[1]

[1]Division of Pulmonary, Allergy, and Critical Care Medicine, Department of Medicine, University of Alabama at Birmingham, Birmingham, AL 35294, USA

[2]Department of Pulmonary, Allergy, and Critical Care Medicine, The Second Affiliated Hospital, Tianjin University of Traditional Chinese Medicine, Tianjin 300150, China

Abstract

Rapid initiation and timely resolution of inflammatory response in macrophages are synergistic events that are known to be equally critical to optimal host defense against pathogen infections. However, the regulation of these processes, in particular by specific cellular metabolic program, has not been well understood. In this study, we found that interferon regulatory factor 2 (IRF2) underwent an early degradation in a proteasome-mediated pathway in LPS treated mouse macrophages, followed by a later recovery of the expression via transactivation. We showed that IRF2 was anti-inflammatory in that knockdown of this protein promoted LPS induced pro-inflammatory mediators. Mechanistically, while IRF2 apparently did not target the proximal cytoplasmic signaling events upon LPS engagements, it inhibited HIF-1α dependent expression of glycolytic genes and thereby cellular glycolysis, sequential events necessary for the IRF2 anti-inflammatory activity. We found that macrophages in endotoxin tolerant state demonstrated deficiency in LPS augmented glycolysis, which was likely caused by failed downregulation of IRF2 and the ensuing upregulation of the glycolytic genes in these cells. In contrast to observations with LPS, knockdown of IRF2 decreased IL-4 induced macrophage alternative activation. The pro-IL-4 activity of IRF2 was dependent on KLF4, a key mediator of the alternative activation, which was transcriptionally induced by IRF2. In conclusion, our data suggest that IRF2 is an important regulator of the pro-inflammatory response in macrophages by controlling HIF-1α dependent glycolytic gene expression and glycolysis. This study also indicates IRF2 as a novel therapeutic target to treat inflammatory disorders associated with dysregulations of macrophage activations.

Address correspondence to: Gang Liu, M.D., Ph.D., Professor of Medicine, Division of Pulmonary, Allergy, and Critical Care Medicine, Department of Medicine, University of Alabama at Birmingham, 901 19th St. So., BMR II 233, Birmingham, Alabama 35294. Tel: 205-975-8932, Fax: 205-934-7437, gangliu@uabmc.edu.
Gang Liu ORCID: 0000-0003-2615-131X

Author contributions:

HC and GL designed the study; HC, SB, SG, NX, and GL performed the experiments and/or analyzed the data; GL supervised the study; HC and GL wrote the manuscript.

Keywords

IRF2; glycolysis; inflammatory response; macrophages polarization; endotoxin tolerance

Introduction

Rapid inflammatory response is a critical host defense against invading microbial pathogens. However, immune response should be also under tight controls in that excessive inflammation often leads to tissue injury and diseases, including acute lung injury (ALI) (1–6). Macrophages are one of the most important inflammatory mediators. This type of cells demonstrates a remarkable plasticity, with the ability to undergo dynamic transitions across distinct functional phenotypes (7–10). The differential activation of macrophages has been the focus of recent studies, particularly with regard to the regulations by transcriptional factors (7, 11).

There have also been emerging concepts that metabolic reprogramming plays a critical role in regulating macrophage activation and immune response (12–15). For example, LPS stimulated macrophages demonstrate enhanced aerobic glycolysis while IL-4 activated cells undertake augmented fatty acid oxidation and glutaminolysis (13, 15–19). More importantly, the newly adopted metabolic programs are essential for macrophages to develop differential activation associated phenotypic traits and functions (12, 13, 16, 17).

The interferon regulatory transcription factor (IRF) family plays a myriad of roles in host responses to bacterial and viral infections (20–22). There have been a number of studies showing that the IRF family members, particularly IRF4 and IRF5, participate in differential macrophage activations (23–25). While it is evident that IRFs can regulate these processes by directly trans-activating phenotypic markers in macrophages, it is less clear if this family participates in metabolic reprogramming and if so, what the role of specific metabolic program is in IRFs mediated macrophage activations.

During our systemic effort to delineate the role of IRF family in inflammatory lung diseases, we found that IRF2 demonstrated unique characteristic distinct from other IRF members. We found that IRF2 underwent early proteasome-mediated degradation, which was necessary for HIF-1α dependent glycolytic gene expression and glycolysis, in LPS treated macrophages. We found that IRF2 was anti-inflammatory and this activity required IRF2 suppression of glycolysis. We also found that IRF2 promoted alternative activation of macrophages by IL-4. Together, our study indicates IRF2 as a new therapeutic target for treating inflammatory disorders associated with dysregulations of macrophage activations.

Materials and Methods

Reagents

PAM3CSK4 was from Invivogen. Mouse recombinant IL-4 was from Peprotech. Mouse recombinant IFN-β was from R&D Systems. Ultra-pure LPS from *Escherichia coli* O111:B4, 2-deoxy-D-glucose (2-DG), cycloheximide (CHX), actinomycin D (ActD) and

MG132 were from Sigma-Aldrich. Chetomin was from Santa Cruz Biotechnology. Bafilomycin A1 was from Cayman Chemical.

Cell line

The mouse macrophage cell line MH-S was purchased from the American Type Culture Collection (ATCC) and cultured according to the ATCC instructions.

Establishment of mouse bone marrow-derived macrophages (BMDMs) and peritoneal macrophages

Mouse BMDMs were derived from bone marrow cells of C57BL/6 mice as previously described (26). Briefly, following erythrocyte lysis, bone marrow cells were cultured in DMEM containing 10% FBS and 50 ng/ml murine macrophage colony-stimulating factor (R&D Systems) for 5 days. The differentiated cells were then split and plated for following experiments. Peritoneal macrophages were elicited in 8-week-old mice by intraperitoneal injection of 1 ml 4% Brewer thioglycollate (Sigma-Aldrich). Peritoneal cells were harvested 4 days later by lavage and plated for 2h, followed by extensive wash to remove non-adherent cells. The adherent cells were used as peritoneal macrophages. The animal protocol was approved by the University of Alabama at Birmingham Institutional Animal Care and Use Committee.

siRNA transfection

siRNA transfection was performed using HiPerFect reagents (Qiagen) according to the manufacturer's instructions. ON-TARGETplus negative control siRNA pool, specific mouse IRF2 siRNA pool and individual IRF2 siRNA oligos, KLF4 siRNA pool, and Accell negative control and IRF2 siRNAs were from Dharmacon.

RNA sequencing (RNA-seq) assay

RNA-seq was performed by the UAB Heflin Center for Genomic Science. RNA-seq data were submitted to Gene Expression Omnibus and are unrestrictedly accessible with accession number GSE106895 (https://www.ncbi.nlm.nih.gov/geo/query/acc.cgi?acc=GSE106895).

Real-time PCR

mRNA levels were determined by real-time PCR using SYBR Green Master Mix Kit (Roche). Primer sequences for mouse genes were: Tubulin α1: sense, 5′ GGATGCTGCCAATAACTATGCTCGT 3′, antisense, 5′ GCCAAAGCTGTGGAAAACCAAGAAG 3′; IRF2: sense, 5′ ATGAAGAGAACGCAGAGGGGAG 3′, antisense, 5′ GCTTGTTGGAGGTGACAAAGGT 3′; IL-1β: sense, 5′ AAGGAGAACCAAGCAACGACAAAATA 3′, antisense, 5′ TTTCCATCTTCTTCTTTGGGTATTGC 3′; iNOS: sense, 5′ ATCTTTGCCACCAAGATGGCCTGG 3′, antisense, 5′ TTCCTGTGCTGTGCTACAGTTCCG 3′; ATF3: sense, 5′ ACACCTCTGCCATCGGATGTCCTCT 3′, antisense, 5′

ATTTCTTTCTCGCCGCCTCCTTTTC 3′; CEBP-′: sense, 5′ AACTTGATTCCTCGTTGCCTCTACTTTC 3′, antisense, 5′ CCGCAAACATTACAATTACTGGCTTTT 3′; HK2: sense, 5′ CTTACCGTCTGGCTGACCAACAC 3′, antisense, 5′ CTCCATTTCCACCTTCATCCTTCT 3′; PFKFB3: sense, 5′ CTGACAAAGGAAGGTGGACAGATTG 3′, antisense, 5′ CCACAACAGTAGGGTCGTCACAGAC 3′; Arg-1: sense, 5′ TGACTGAAGTAGACAAGCTGGGGAT 3′, antisense, 5′ CGACATCAAAGCTCAGGTGAATCGG 3′; YM-1: sense, 5′ ATGAAGCATTGAATGGTCTGAAAG 3′, antisense, 5′ TGAATATCTGACGGTTCTGAGGAG 3′; FIZZ1: sense, 5′ AGGTCAAGGAACTTCTTGCCAATCC 3′, antisense, 5′ AAGCACACCCAGTAGCAGTCATCCC 3′; MGL1: sense, 5′ GCTTCGAAAAAGGGATCAGTTCTCT 3′, antisense, 5′ CTCTTCTCCACTGTGCTCTCCAGAG 3′; KLF4: sense, 5′ TACCCTCCTTTCCTGCCAGACCA 3′, antisense, 5′ GCCACGACCTTCTTCCCCTCTTT 3′. To calculate fold change in the expression of these genes, ΔCt = Ct of Tubulin - Ct of individual genes was first obtained. ΔΔCt = ΔCt of treated groups - ΔCt of untreated control groups was then obtained. Fold change was calculated as $2^{\Delta\Delta Ct}$, with control groups as 1 fold.

Western blotting

Western blotting was performed as previously described (27). Mouse anti-α-tubulin antibody was from Sigma-Aldrich. Rabbit anti-IRF2, Lamin B1, Arg-1, and iNOS antibodies were from Santa Cruz Biotechnology. Rabbit anti-HK2, p65, p-p65, ERK1/2, p-ERK1/2, p38, p-p38, JNK, p-JNK, IκBα, KLF4 and STAT6 antibodies were from Cell Signaling Technology. Rabbit anti-HIF-1a antibody was from Novus Biologicals. Rabbit anti-PFKFB3 antibody was from Abcam. Goat anti-mIL-1β antibody was from R&D Systems.

Enzyme-linked immunosorbent assay (ELISA)

Levels of secreted YM-1 in cell culture supernatants were determined using DuoSet ELISA development kits (R&D Systems) according to the manufacturer's instructions.

Bacteria killing assay

Bacterial killing assay was performed as described previously (26, 28). Briefly, 0.1×10^6 cfu/ml *Escherichia coli* (BL21DE3pLysS) were added to macrophages in 96-well plates and incubated at 37 °C for 1 h. Supernatants were serially diluted and plated on Luria broth-agar plates. The plates were incubated overnight at 37 °C, and bacterial colonies were counted. Data were presented as colony-forming unit (cfu)/ml.

Real-time cell metabolism assay

XF-24 Extracellular Flux Analyzer (Seahorse Bioscience) was used for real-time recording of extracellular acidification rate (ECAR). Briefly, BMDMs were seeded in Seahorse XF-24

microplates (1.5×10^5 cells/well), and treated with or without 100 ng/ml LPS for 6 h. Before analysis, the cells were incubated in ECAR media for 1 h at 37°C in room air. Cells were sequentially treated with 10 mM glucose, 2 μg/ml oligomycin, and 5 mM 2-DG. Real-time ECAR were recorded according to the manufacturer's manual.

Glucose consumption assay

Glucose levels in the cell culture supernatants were determined using a glucose colorimetric/fluorometric assay kit (Biovision) according the manufacturer's instructions. Glucose consumption was calculated as (glucose level of fresh medium-glucose levels of supernatants)/μg protein/incubation hours.

Extracellular lactate assay

Extracellular levels of lactate were determined using lactate assay kit (BioVision) according to the manufacturer's instructions.

Chromatin immunoprecipitation (ChIP) assay

ChIP assays were performed as previously described (29). Briefly, BMDMs were fixed with 1% formaldehyde in PBS for 10 min and collected in RIPA buffer. Genomic DNA was then sheared by sonication to length around 200–500 bp. One percent of the cell extracts was taken as input, and the rest of the extracts was incubated with either rabbit anti-HIF-1α antibody, anti-KLF4 antibody, or rabbit IgG overnight, followed by precipitation with protein G agarose beads (Invitrogen). Genomic DNA in the immunocomplexes was purified using Qiagen miniprep columns (Qiagen). Primer sequences to specifically amplify the *HK2* promoter or *PFKFB3* promoter region spanning the putative HIF-1α binding site/hypoxia-response element (HRE) were: *HK2*-HRE: sense, 5′ GTTGAGCTACAATTAAGATGAGAATCA 3′, antisense, 5′ CCCAAGCAGGCGGCGGGAGAGA 3′; *PFKFB3*-HRE: sense, 5′ GTGTGTGTGTGTAGGGGTGGAGGA 3′, antisense, 5′ ACGTGGAGAGAAGGGTGGGCAAGG 3′. Primer sequences to amplify the *KLF4* promoter region spanning the putative IRF2 binding elements (IRF-E) were: *KLF4*-IRF-E-#1 sense, 5′ GGTAGTGGGGAATGGGAAAAGGAGT 3′, antisense, 5′ ATAAAGAGGTGAAGCGGCGAGGTAA 3′; *KLF4*-IRF-E-#2 sense, 5′ AGGTGTTCTTTTTGTTGTTCCTTTGT 3′, antisense, 5′ TTCATCCTTTCTCTTGGTTTTGGC 3′.

Statistical analysis

One-way ANOVA followed by the Bonferroni test was used for multiple group comparisons. The Student's *t* test was used for comparison between two groups. $p<0.05$ was considered statistically significant.

Results

IRF2 undergoes early degradation in response to LPS stimulation in macrophages

To determine the role of IRF2 in inflammatory response, we initially characterized its expression in LPS treated macrophages. As shown in Figure 1A, the protein level of IRF2 was rapidly decreased prior to its recovery at 6h after LPS stimulation. IRF2 protein level in macrophages treated with the TLR2 ligand Pam3CSK4 demonstrated a similar pattern of alterations, although at a delayed kinetics (Figure 1B). Intriguingly, IRF2 reduction appeared coincident with the induction of the pro-inflammatory cytokine IL-1β in LPS and Pam3CSK4 treated cells (Figures 1A–1B). To determine if the decrease in the IRF2 protein level was caused by a downregulated IRF2 transcription, we examined IRF2 mRNA levels and found surprisingly that IRF2 was transcriptionally upregulated in LPS treated macrophages (Figure 1C). In the aggregate, these data clearly suggest that IRF2 expression undergoes a dynamic regulation at both the transcriptional and post-transcriptional levels in response to LPS stimulation. To delineate the mechanism underlying the early decline in IRF2 protein in LPS treated macrophages, we examined its stability by blocking cellular translation and found that IRF2 was short-lived in that nearly half of the protein was degraded within three hours (Figure 1D). More importantly, LPS treatment promoted IRF2 degradation (Figure 1D). Of note, both findings resembled what observed with the principal anti-inflammatory mediator IκBα in LPS treated macrophages (Figure 1D) (30). Next, we demonstrated that the physiological turnover of the IRF2 protein was mediated by proteasomes as the proteasome inhibitor MG132 completely blocked this process (Figure 1E). The proteasome dependent degradation was found to be solely responsible for the LPS induced early downregulation of the IRF2 protein because MG132, but not the lysosome inhibitor Bafilomycin A1, completely abolished this phenomenon (Figures 1F–1G). As expected, autophagy mediator LC3-II was accumulated because of lysosome inhibition in Bafilomycin A1 treated cells (Figure 1G). Additionally, to determine if LPS induced IRF2 transcription accounted for the later restoration of the protein expression, we inhibited cellular transcription with actinomycin D and found that the IRF2 protein level failed to recover when transcription was halted in LPS treated macrophages (Figure 1H). Collectively, these data suggest that the expression of IRF2 bears the trait typical of that of key inflammatory regulators that function in a negative feed-back manner in response to LPS.

IRF2 knockdown promotes inflammatory response in LPS treated macrophages

The resemblance of IRF2 expression dynamics to that of typical negative regulators in inflamed macrophages prompted us to ask if this protein also functioned in the similar manner to regulate immune response (2, 30). To test this hypothesis, we knocked down IRF2 in BMDMs and examined the pro-inflammatory cytokines and mediators in these cells after LPS stimulation. We found that IRF2 knockdown significantly augmented the LPS induced expression of IL-1β, iNOS, TNF-α, and IL-12 at both mRNA and protein levels (Figures 2A–2D and data not shown). The increased expression of the pro-inflammatory mediators was also observed in LPS treated peritoneal macrophages and macrophage line MH-S cells with IRF2 knockdown, suggesting a general role of IRF2 in macrophages in response to LPS (Supplemental Figures 1A–1B). To rule out the possibility that the effect of IRF2

knockdown in LPS treated macrophages was caused by any off-target effect from a single IRF2 siRNA, we replicated the experiments with siRNAs separately targeting two independent locations in the IRF2 transcripts. As shown in Supplemental Figure 1C, both siRNAs efficiently knocked down IRF2. More importantly, both siRNAs enhanced the expression of IL-1β and iNOS to the same levels, indicative of the specificity of the findings with IRF2 knockdown. This conclusion was further reinforced after achieving similar results using a different type of IRF2 siRNA molecules, Accell siRNAs, which required drastically reduced transfection reagents (Supplemental Figure 1D). There was also evidence showing that IRF2 could competitively inhibit IRF1 mediated type I interferon (IFN) response that is known to be present in LPS treated macrophages (1). To determine the role of IRF1 and the resulting IFN activation in the IRF2 anti-inflammatory activity, we co-treated the macrophages with IFN-β. As expected, IFN-β significantly induced IRF1 dependent expression of ISG15 and Gbp2 (Supplemental Figure 2A). However, IFN-β had no effect on the increased expression of IL-1β and iNOS in LPS treated IRF2 knockdown cells (Supplemental Figures 2B–2C). Together, these data indicate that the anti-inflammatory effect of IRF2 is not achieved through regulating IRF1 associated type I IFN response. Additionally, as functional activities of inflamed macrophages, such as bacteria killing capability, are often commensurate with the levels of inflammatory response (10, 31), we investigated if IRF2 knockdown promoted such activities of the cells. Consistent with LPS induced expression of iNOS, we found that the bactericidal activity of LPS treated macrophages was significantly increased when IRF2 was knocked down (Figures 2E–2F). Collectively, the results suggest that IRF2 is a negative regulator of immune response in macrophages. Moreover, it appears that the early degradation of the IRF2 protein is to facilitate macrophages mounting swift pro-inflammatory reaction to microbial infections.

IRF2 knockdown has no effects on proximal signaling events upon LPS stimulation or the expression of several key regulators of LPS induced inflammation in macrophages

We had demonstrated that knockdown of IRF2 promoted the inflammatory response to LPS in macrophages. Next we sought for the mechanisms underlying these observations. We first examined the principal signaling cascade upon LPS stimulation, which includes phosphorylation and activation of NF-κB subunit p65 and MAPKs (1, 3). As shown in Figure 3A, IRF2 knockdown exerted no effect on the phosphorylation of p65, ERK1/2, p38 or JNK in LPS treated macrophages, suggesting that the immediate signaling events downstream LPS engaging with its receptor TLR4 were not the targets of IRF2. Furthermore, as an essential step of the LPS induced pro-inflammatory mediators, including IL-1β and iNOS, p65 bindings to the promoters of these genes remained unchanged when IRF2 was knocked down (Figure 3B). Additionally, we examined if IRF2 had a role in the expression of ATF3 and CEBP-δ, two well recognized key regulators of the LPS induced inflammatory response (32–34), and found that the level of neither ATF3 nor CEBP-δ was affected in the naïve and LPS treated macrophages with IRF2 knockdown (Figures 3C–3D). Taken together, these data suggest that IRF2 may not have a direct role in LPS induced proximal signaling cascade. These results also indicate that IRF2 does not act via the investigated regulators, i.e. ATF3 and CEBP-δ, that have a major role in LPS induced inflammatory responses.

IRF2 knockdown promotes glycolysis in macrophages

The lack of effects of IRF2 knockdown on the LPS induced cytoplasmic signaling events led us to reason that IRF2, a transcriptional factor itself, may regulate inflammatory responses at the transcriptional level. Therefore, we performed RNA sequencing analyses on macrophages with or without IRF2 knockdown. Among genes that were upregulated in the IRF2 knockdown cells, we noticed a clear presence of a number of glycolytic mediators, such as HK2 and PFKFB3 (Figure 4A). As it had been increasingly recognized that augmented aerobic glycolysis was essential to the development of inflamed phenotype in LPS treated macrophages (12, 13, 18), we hypothesized that IRF2 promoted inflammation by boosting glycolysis in these cells. At first, we validated the RNA sequencing results by real-time PCR and showed that the expression of HK2 and PFKFB3 was increased in the naive macrophages with IRF2 knockdown (Figure 4B). We also found that LPS induction of these genes was further augmented in IRF2 knockdown cells (Figures 4B–4D). To determine the metabolic consequence of the elevated glycolytic mediators, we examined ECAR, a surrogate of lactate production rate and intracellular glycolytic level, using Seahorse Bioanalyzer. We found that ECAR in naïve IRF2 knockdown macrophages was markedly increased compared to that in control siRNA transfected cells (Figure 4E). Furthermore, LPS augmented ECAR was again enhanced in the macrophages with IRF2 knockdown compared to that in the control cells (Figure 4E). These data were in line with the greater levels of lactate productions and glucose consumptions found in the naïve and LPS treated macrophages with IRF2 knockdown compared with those in control cells (Figures 4F–4G). Collectively, our findings suggest that IRF2 suppresses glycolysis in macrophages by inhibiting the expression of glycolytic mediators. To further determine if the augmented glycolysis observed in IRF2 knockdown macrophages accounted for the aggravated LPS induced inflammatory responses in these cells, we blocked cellular glycolysis with hexokinase inhibitor 2-DG and found that the increases in the expression of pro-inflammatory mediators in IRF2 knockdown macrophages were abolished (Figure 4H). In summary, our data suggest that IRF2 suppresses inflammation by inhibiting the expression of glycolytic genes and thereby cellular glycolysis.

IRF2 regulated glycolysis and inflammation are dependent on HIF-1α in macrophages

As hypoxia-inducible factor 1α (HIF-1α) is the master regulator of glycolytic gene expression and glycolysis (12, 13, 35), we asked if HIF-1α played a role in the IRF2 modulated events. First, we found that the augmentation in the LPS induced glycolytic genes HK2 and PFKFB3 in IRF2 knockdown macrophages was abrogated when the cells were treated with specific HIF-1α inhibitor chetomin (Figure 5A). In line with this observation, the elevated expression of the pro-inflammatory mediators IL-1β and iNOS after IRF2 was knocked down was also abolished by chetomin in LPS treated macrophages (Figure 5B). Together, these data suggest that IRF2 regulated glycolytic gene expression and inflammation is mediated by HIF-1α. To investigate the mechanism by which IRF2 regulated these HIF-1α mediated events, we examined the levels of HIF-1α and found unexpectedly that HIF-1α expression in both naïve and LPS treated macrophages remained largely unaffected by IRF2 knockdown (Figure 5C), suggesting that IRF2 may be involved in the transcriptional activity of HIF-1α. To test this hypothesis, we determined HIF-1α binding by ChIP assays to the promoters of its targets, one of the critical steps that decide

the transactivation of these genes. As shown in Figure 5D, there were significant increases in the bindings of HIF-1α to the promoters of *HK2* and *PFKFB3* upon LPS stimulation. More importantly, the HIF-1α bindings were further enhanced in LPS treated IRF2 knockdown cells (Figure 5D). In all, these results indicate that IRF2 inhibits inflammation by suppressing HIF-1α dependent expression of glycolytic genes and glycolysis.

IRF2 knockdown relieves endotoxin tolerance in macrophages

As a number of anti-inflammatory regulators that function by the negative feed-back mechanism also participate in endotoxin tolerance, itself a continuation of acute immune response (36), we asked if IRF2 had such an activity. To do this, macrophages were treated with LPS for 24 h (1st LPS) to induce tolerance. The cells were cultured in fresh media that contained or not LPS for 6 h (2nd LPS). We found that tolerant macrophages were nearly unresponsive to 2nd LPS stimulation as they expressed minimal pro-inflammatory mediators IL-1β and iNOS (Figure 6A). However, the LPS tolerant state was partially relieved in macrophages when IRF2 was knocked down as these cells produced markedly more IL-1β and iNOS (Figure 6B). These data suggest that IRF2 is required for the establishment of endotoxin tolerance in macrophages. To delineate the underlying mechanism, we examined IRF2 expression in the tolerant macrophages. In contrast to the LPS induced early degradation of the IRF2 protein in the naïve macrophages, IRF2 levels were largely unchanged at the same early time point of LPS treatment of the tolerant cells (Figure 6C). Given that IRF2 inhibited glycolytic gene expression, these data suggest that the failure of IRF2 downregulation may hinder the upregulation of these genes and the ensuing augmentation of glycolysis in LPS treated tolerant macrophages. As anticipated, we did find that LPS induction of glycolytic genes HK2 and PFKFB3 was literally eliminated in tolerant macrophages compared to naïve cells (Figure 6D). However, the expression of HK2 and PFKFB3 was significantly increased in tolerant macrophages when IRF2 was knocked down (Figure 6E). Consistent with this finding, glycolysis, as reflected by ECAR and lactate production with and without 2nd LPS treatment, was markedly augmented in tolerant macrophages with IRF2 knockdown (Figures 6F–6G). Furthermore, we found that blocking glycolysis by 2-DG completely abolished the partial recovery of the LPS sensitivity in tolerant macrophages with IRF2 knockdown (Figure 6H). In summary, these data indicate that IRF2 suppression of glycolysis is required for endotoxin tolerance in macrophages.

IRF2 participates in alternative activation of macrophages by IL-4

Many negative regulators of inflammation participated in alternative macrophage activation, which, together with the pro-inflammatory one, occupied the two opposite spectrums of macrophage phenotype (37). As we had demonstrated that IRF2 was a negative regulator of pro-inflammatory response, we next asked if this transcription factor also played a role in alternative activation of macrophages. First, we investigated IRF2 levels in IL-4 treated macrophages (M(IL-4)). As shown in Figures 7A–7C, IL-4 increased the expression of IRF2 at both the RNA and protein levels. These data suggest that IRF2 may regulate IL-4 induced macrophage activation. Additionally, There was elevated levels of IRF2 in the nuclei of IL-4 treated macrophages (Figure 7D), indicative of its location of action in regulation of M(IL-4) activation.

We then determined if IRF2 participated in M(IL-4) activation. As shown in Figures 7E–7H, there were significant decreases in IL-4 induced markers of alternatively activated macrophages at both mRNA and protein levels when IRF2 was knocked down. These data suggest that, in contrast to being anti-inflammatory, IRF2 promotes macrophage alternative activation.

IRF2 promotion of alternative activation of macrophages by IL-4 is KLF4-dependent

To delineate the mechanism by which IRF2 promoted IL-4 induced alternative activation of macrophages, we again interrogated the RNA sequencing results and found that KLF4, a crucial regulator of M(IL-4) activation (38), was downregulated in macrophages with IRF2 knockdown. We validated this finding by real-time PCR. As shown in Figure 8A, KLF4 transcription was decreased when IRF2 was knocked down. Furthermore, IL-4 induced KLF4 was also diminished in IRF2 knockdown macrophages (Figure 8A). These data were consistent with the attenuated induction of the KLF4 protein by IL-4 in macrophages with IRF2 knockdown, although KLF4 at basal levels was not detectable by the antibody (Figure 8B). We further determined how IRF2 transcriptionally regulated KLF4. We found that there were three typical IRF2 binding sites within 2 kb upstream the KLF4 transcription start site (Figure 8C). We performed ChIP assays with anti-IRF2 antibody pull-down and examined IRF2 bindings to the predicted sites. As shown in Figure 8C, we found that IRF2 binding to these sites was significantly increased in IL-4 activated macrophages, suggesting that IRF2 directly mediates IL-4 induction of KLF4. We next confirmed the pro-M(IL-4) activity of KLF4 in that we found that the expression of alternatively activated macrophage markers was markedly reduced when KLF4 was knocked down (Figures 8D–8E). In light of these findings, we asked if the promotion of M(IL-4) activation by IRF2 was dependent on its induction of KLF4. To test this hypothesis, we determined the effect of IRF2 in macrophages with or without KLF4 knockdown. As shown in Figure 8F, the attenuation of M(IL-4) activation by IRF2 siRNAs was largely abolished in macrophages with prior KLF4 knockdown. In addition, consistent with the previous finding that KLF4 was a key co-activator for IL-4 induced STAT6 transcriptional activation (38), we found that STAT6 bindings to the promoters of alternative macrophage markers, but not its phosphorylation or nuclear translocation, were diminished in IRF2 knockdown macrophages upon IL-4 stimulation (Supplemental Figures 3A–3C). In all, these data suggest that IRF2 promotes alternative activation of macrophages by transactivation of KLF4.

Discussion

The IRF family members have been shown to demonstrate a versatility of activities in regulating immune responses (20–25). However, these investigations were generally focused on mechanisms at the transcriptional and epigenetic levels. In this study, we not only found that IRF2 participated in the differential activation of macrophages, but also established the causal link between IRF2 regulated glycolysis and its anti-inflammatory activity. Our study has thus reinforced the increasingly recognized role of cellular metabolism in the regulation of immunological response, which has been manifested in a number of immune dysregulation associated diseases. Among those ample evidence is the necessity of glycolytic homeostasis in the maintenance of a balanced immune system. Either hyper- or

hypo-glycolytic responses in various immune cells, including macrophages, monocytes, dendritic cells, and T lymphocytes, have been implicated in clinically relevant immunological pathologies, such as sepsis and diabetes (39–45). This has led to the concept that modulating glycolysis to experimentally treat immune disorders (46, 47). Given our findings revealing the intersection of IRF2 and glycolysis, this study has also indicated potential novel therapeutic targets in dealing with this group of diseases.

We have shown that IRF2 differentially impacts the recruitments of HIF-1α and KLF4 to the promoters of their respective target genes in that IRF2 inhibited the bindings of HIF-1α, but enhanced those of KLF4 in activated macrophages. However, the mechanism by which IRF2 achieves such specificity remains to be elucidated. One appealing hypothesis is that IRF2 may undergo distinct post-translational modifications in differentially activated macrophages. These unique modifications may dictate the interaction of IRF2 with either transcriptional co-activators or co-repressors, which in turn may determine the accessibility of the promoters of individual target genes to these specific transcription factors and the ensuing transcriptional robustness. Therefore, further studies focusing on identification of IRF2 modifications appear to be warranted.

Additionally, post-translational modifications are also likely involved in the early degradation of IRF2 in LPS treated macrophages, similar to that observed with IκBα (2, 30). These findings continuingly advance our understanding that this type of maneuver is a commonly harnessed mechanism by which immune cells overcome early hurdles in order to launch a robust inflammation that is needed to combat pathological microbial invasion. Furthermore, the observation that the recovery of the IRF2 expression via elevated transcription in later stage of inflammatory response seems to place IRF2 squarely into the category of inflammation rheostats. This group of molecules has been frequently found to be critical to immune homeostasis, and dysregulations of which are known causes for inflammatory disorders (5, 6, 48). Given the anti-inflammatory role of IRF2 and its pro-alternative macrophage activation, it is surely enticing to delineate its role *in vivo* in both type I and type II inflammation animal models. Besides, we will also gain mechanistic insight through investigating IRF2 levels and genetic variants in human immune diseases, such as acute lung injury and asthma.

Also importantly, the participation of IRF2 in endotoxin tolerance, a state of immunoparalysis that is a primary cause for secondary infections in sepsis patients, seems to justify the comparison of the dynamics of IRF2 expression in those subjects at the time of admission and recovery. While recent studies showed that macrophages in tolerant state were characteristic of metabolic catastrophe, including defects in glycolysis, it remained unclear of the causes behind these dysregulations (17, 39, 49). Our study not only confirmed the contribution of glycolytic hypo-responsiveness to endotoxin tolerance, but also did it shed light on the underlying mechanism, e.g. the absence of IRF2 degradation leading to failure of glycolytic gene induction and substantial glycolytic augmentation in tolerant macrophages, which is metabolically required for robust inflammatory response. Therefore, our findings identify a new therapeutic target for treating disorders associated with immunoparalysis.

It should be noted that early studies also showed that IRF2 deficient cells or mice were protective from LPS challenge (50–52). These findings, although lacking mechanistic details, seem inconsistent with our results and some other reports that IRF2 was antagonistic of type I IFN response (22, 53, 54). However, these discrepancies may arise from a series of scenarios that could occur in global knockout animals, including differences in genetic background between the knockout mice and the wild-type counterparts, potential phenotypic alternations caused by constitutional ablation of IRF2, and likelihood of unintended deletion of functional non-coding sequences, such as miRNAs, which are located at the same locus as IRF2. Regardless, our conclusion was firmly based on multiple genetic and pharmaceutical approaches, such as replicating experiments using siRNAs with independent sequences to target the same gene expression and confirming the hierarchy of each regulatory event with specific inhibitors.

Finally, the current study is meticulous in delineating IRF2 regulation of glycolysis and glycolysis dependent immune response in macrophages. The rationale for such an emphasis on one type of metabolic pathways was not a bias, but rather informed by our RNA sequencing analysis that revealed the predominant targets of IRF2 being genes associated with glycolysis. Nevertheless, given the rapidly accumulating evidence clearly showing that other core metabolisms, such as fatty acid oxidation and glutaminolysis (13, 15–19), are also involved in the activation of a variety of immune cells, there is a good likelihood that IRF2 may interact with those metabolic elements, either directly or indirectly, to control the response of macrophages in pathological settings. This hypothesis remains an evidently interesting point in future studies.

Supplementary Material

Refer to Web version on PubMed Central for supplementary material.

Acknowledgments

This work was supported by NIH grants HL135830 and HL114470.

References

1. Akira S, Uematsu S, Takeuchi O. Pathogen recognition and innate immunity. Cell. 2006; 124:783–801. [PubMed: 16497588]
2. Kondo T, Kawai T, Akira S. Dissecting negative regulation of Toll-like receptor signaling. Trends Immunol. 2012; 33:449–458. [PubMed: 22721918]
3. Takeuchi O, Akira S. Pattern recognition receptors and inflammation. Cell. 2010; 140:805–820. [PubMed: 20303872]
4. Ware LB, Matthay MA. The acute respiratory distress syndrome. N Engl J Med. 2000; 342:1334–1349. [PubMed: 10793167]
5. Kotas ME, Medzhitov R. Homeostasis, inflammation, and disease susceptibility. Cell. 2015; 160:816–827. [PubMed: 25723161]
6. Nathan C, Ding A. Nonresolving inflammation. Cell. 2010; 140:871–882. [PubMed: 20303877]
7. Lawrence T, Natoli G. Transcriptional regulation of macrophage polarization: enabling diversity with identity. Nat Rev Immunol. 2011; 11:750–761. [PubMed: 22025054]
8. Murray PJ, Wynn TA. Obstacles and opportunities for understanding macrophage polarization. J Leukoc Biol. 2011; 89:557–563. [PubMed: 21248152]

9. Sica A, Mantovani A. Macrophage plasticity and polarization: in vivo veritas. J Clin Invest. 2012; 122:787–795. [PubMed: 22378047]
10. Mosser DM, Edwards JP. Exploring the full spectrum of macrophage activation. Nat Rev Immunol. 2008; 8:958–969. [PubMed: 19029990]
11. Tugal D, Liao X, Jain MK. Transcriptional control of macrophage polarization. Arterioscler Thromb Vasc Biol. 2013; 33:1135–1144. [PubMed: 23640482]
12. Galvan-Pena S, O'Neill LA. Metabolic reprograming in macrophage polarization. Front Immunol. 2014; 5:420. [PubMed: 25228902]
13. Tannahill GM, Curtis AM, Adamik J, Palsson-McDermott EM, McGettrick AF, Goel G, Frezza C, Bernard NJ, Kelly B, Foley NH, Zheng L, Gardet A, Tong Z, Jany SS, Corr SC, Haneklaus M, Caffrey BE, Pierce K, Walmsley S, Beasley FC, Cummins E, Nizet V, Whyte M, Taylor CT, Lin H, Masters SL, Gottlieb E, Kelly VP, Clish C, Auron PE, Xavier RJ, O'Neill LA. Succinate is an inflammatory signal that induces IL-1beta through HIF-1alpha. Nature. 2013; 496:238–242. [PubMed: 23535595]
14. Rodriguez-Prados JC, Traves PG, Cuenca J, Rico D, Aragones J, Martin-Sanz P, Cascante M, Bosca L. Substrate fate in activated macrophages: a comparison between innate, classic, and alternative activation. J Immunol. 2010; 185:605–614. [PubMed: 20498354]
15. Nomura M, Liu J, Rovira, Gonzalez-Hurtado E, Lee J, Wolfgang MJ, Finkel T. Fatty acid oxidation in macrophage polarization. Nat Immunol. 2016; 17:216–217. [PubMed: 26882249]
16. Huang SC, Everts B, Ivanova Y, O'Sullivan D, Nascimento M, Smith AM, Beatty W, Love-Gregory L, Lam WY, O'Neill CM, Yan C, Du H, Abumrad NA, Urban JF Jr, Artyomov MN, Pearce EL, Pearce EJ. Cell-intrinsic lysosomal lipolysis is essential for alternative activation of macrophages. Nat Immunol. 2014; 15:846–855. [PubMed: 25086775]
17. Liu PS, Wang H, Li X, Chao T, Teav T, Christen S, Di Conza G, Cheng WC, Chou CH, Vavakova M, Muret C, Debackere K, Mazzone M, Huang HD, Fendt SM, Ivanisevic J, Ho PC. alpha-ketoglutarate orchestrates macrophage activation through metabolic and epigenetic reprogramming. Nat Immunol. 2017; 18:985–994. [PubMed: 28714978]
18. Freemerman AJ, Johnson AR, Sacks GN, Milner JJ, Kirk EL, Troester MA, Macintyre AN, Goraksha-Hicks P, Rathmell JC, Makowski L. Metabolic reprogramming of macrophages: glucose transporter 1 (GLUT1)-mediated glucose metabolism drives a proinflammatory phenotype. J Biol Chem. 2014; 289:7884–7896. [PubMed: 24492615]
19. Tan Z, Xie N, Banerjee S, Cui H, Fu M, Thannickal VJ, Liu G. The monocarboxylate transporter 4 is required for glycolytic reprogramming and inflammatory response in macrophages. J Biol Chem. 2015; 290:46–55. [PubMed: 25406319]
20. Medzhitov R. Toll-like receptors and innate immunity. Nat Rev Immunol. 2001; 1:135–145. [PubMed: 11905821]
21. Ikushima H, Negishi H, Taniguchi T. The IRF family transcription factors at the interface of innate and adaptive immune responses. Cold Spring Harb Symp Quant Biol. 2013; 78:105–116. [PubMed: 24092468]
22. Taniguchi T, Ogasawara K, Takaoka A, Tanaka N. IRF family of transcription factors as regulators of host defense. Annu Rev Immunol. 2001; 19:623–655. [PubMed: 11244049]
23. Takaoka A, Yanai H, Kondo S, Duncan G, Negishi H, Mizutani T, Kano S, Honda K, Ohba Y, Mak TW, Taniguchi T. Integral role of IRF-5 in the gene induction programme activated by Toll-like receptors. Nature. 2005; 434:243–249. [PubMed: 15665823]
24. Satoh T, Takeuchi O, Vandenbon A, Yasuda K, Tanaka Y, Kumagai Y, Miyake T, Matsushita K, Okazaki T, Saitoh T, Honma K, Matsuyama T, Yui K, Tsujimura T, Standley DM, Nakanishi K, Nakai K, Akira S. The Jmjd3-Irf4 axis regulates M2 macrophage polarization and host responses against helminth infection. Nat Immunol. 2010; 11:936–944. [PubMed: 20729857]
25. Huang SC, Smith AM, Everts B, Colonna M, Pearce EL, Schilling JD, Pearce EJ. Metabolic Reprogramming Mediated by the mTORC2-IRF4 Signaling Axis Is Essential for Macrophage Alternative Activation. Immunity. 2016; 45:817–830. [PubMed: 27760338]
26. Banerjee S, Xie N, Cui H, Tan Z, Yang S, Icyuz M, Abraham E, Liu G. MicroRNA let-7c regulates macrophage polarization. J Immunol. 2013; 190:6542–6549. [PubMed: 23667114]

27. Liu G, Park YJ, Abraham E. Interleukin-1 receptor-associated kinase (IRAK) -1-mediated NF-kappaB activation requires cytosolic and nuclear activity. FASEB J. 2008; 22:2285–2296. [PubMed: 18276832]
28. Bystrom J, Evans I, Newson J, Stables M, Toor I, van Rooijen N, Crawford M, Colville-Nash P, Farrow S, Gilroy DW. Resolution-phase macrophages possess a unique inflammatory phenotype that is controlled by cAMP. Blood. 2008; 112:4117–4127. [PubMed: 18779392]
29. Cui H, Xie N, Tan Z, Banerjee S, Thannickal VJ, Abraham E, Liu G. The human long noncoding RNA lnc-IL7R regulates the inflammatory response. Eur J Immunol. 2014; 44:2085–2095. [PubMed: 24723426]
30. Finco TS, Baldwin AS. Mechanistic aspects of NF-kappa B regulation: the emerging role of phosphorylation and proteolysis. Immunity. 1995; 3:263–272. [PubMed: 7552992]
31. Shiloh MU, MacMicking JD, Nicholson S, Brause JE, Potter S, Marino M, Fang F, Dinauer M, Nathan C. Phenotype of mice and macrophages deficient in both phagocyte oxidase and inducible nitric oxide synthase. Immunity. 1999; 10:29–38. [PubMed: 10023768]
32. Medzhitov R, Horng T. Transcriptional control of the inflammatory response. Nat Rev Immunol. 2009; 9:692–703. [PubMed: 19859064]
33. Litvak V, Ramsey SA, Rust AG, Zak DE, Kennedy KA, Lampano AE, Nykter M, Shmulevich I, Aderem A. Function of C/EBPdelta in a regulatory circuit that discriminates between transient and persistent TLR4-induced signals. Nat Immunol. 2009; 10:437–443. [PubMed: 19270711]
34. Gilchrist M, Thorsson V, Li B, Rust AG, Korb M, Roach JC, Kennedy K, Hai T, Bolouri H, Aderem A. Systems biology approaches identify ATF3 as a negative regulator of Toll-like receptor 4. Nature. 2006; 441:173–178. [PubMed: 16688168]
35. Nizet V, Johnson RS. Interdependence of hypoxic and innate immune responses. Nat Rev Immunol. 2009; 9:609–617. [PubMed: 19704417]
36. Biswas SK, Lopez-Collazo E. Endotoxin tolerance: new mechanisms, molecules and clinical significance. Trends Immunol. 2009; 30:475–487. [PubMed: 19781994]
37. Liu G, Abraham E. MicroRNAs in immune response and macrophage polarization. Arterioscler Thromb Vasc Biol. 2013; 33:170–177. [PubMed: 23325473]
38. Liao X, Sharma N, Kapadia F, Zhou G, Lu Y, Hong H, Paruchuri K, Mahabeleshwar GH, Dalmas E, Venteclef N, Flask CA, Kim J, Doreian BW, Lu KQ, Kaestner KH, Hamik A, Clement K, Jain MK. Kruppel-like factor 4 regulates macrophage polarization. J Clin Invest. 2011; 121:2736–2749. [PubMed: 21670502]
39. Cheng SC, Scicluna BP, Arts RJ, Gresnigt MS, Lachmandas E, Giamarellos-Bourboulis EJ, Kox M, Manjeri GR, Wagenaars JA, Cremer OL, Leentjens J, van der Meer AJ, van de Veerdonk FL, Bonten MJ, Schultz MJ, Willems PH, Pickkers P, Joosten LA, van der Poll T, Netea MG. Broad defects in the energy metabolism of leukocytes underlie immunoparalysis in sepsis. Nat Immunol. 2016; 17:406–413. [PubMed: 26950237]
40. Krawczyk CM, Holowka T, Sun J, Blagih J, Amiel E, DeBerardinis RJ, Cross JR, Jung E, Thompson CB, Jones RG, Pearce EJ. Toll-like receptor-induced changes in glycolytic metabolism regulate dendritic cell activation. Blood. 2010; 115:4742–4749. [PubMed: 20351312]
41. Chang CH, Curtis JD, Maggi LB Jr, Faubert B, Villarino AV, O'Sullivan D, Huang SC, van der Windt GJ, Blagih J, Qiu J, Weber JD, Pearce EJ, Jones RG, Pearce EL. Posttranscriptional control of T cell effector function by aerobic glycolysis. Cell. 2013; 153:1239–1251. [PubMed: 23746840]
42. Palmer CS, Anzinger JJ, Zhou J, Gouillou M, Landay A, Jaworowski A, McCune JM, Crowe SM. Glucose transporter 1-expressing proinflammatory monocytes are elevated in combination antiretroviral therapy-treated and untreated HIV+ subjects. J Immunol. 2014; 193:5595–5603. [PubMed: 25367121]
43. Everts B, Amiel E, Huang SC, Smith AM, Chang CH, Lam WY, Redmann V, Freitas TC, Blagih J, van der Windt GJ, Artyomov MN, Jones RG, Pearce EL, Pearce EJ. TLR-driven early glycolytic reprogramming via the kinases TBK1-IKKvarepsilon supports the anabolic demands of dendritic cell activation. Nat Immunol. 2014; 15:323–332. [PubMed: 24562310]
44. van Diepen JA, Thiem K, Stienstra R, Riksen NP, Tack CJ, Netea MG. Diabetes propels the risk for cardiovascular disease: sweet monocytes becoming aggressive? Cell Mol Life Sci. 2016; 73:4675–4684. [PubMed: 27469259]

45. Nishizawa T, Kanter JE, Kramer F, Barnhart S, Shen X, Vivekanandan-Giri A, Wall VZ, Kowitz J, Devaraj S, O'Brien KD, Pennathur S, Tang J, Miyaoka RS, Raines EW, Bornfeldt KE. Testing the role of myeloid cell glucose flux in inflammation and atherosclerosis. Cell Rep. 2014; 7:356–365. [PubMed: 24726364]

46. Arts RJW, Carvalho A, La Rocca C, Palma C, Rodrigues F, Silvestre R, Kleinnijenhuis J, Lachmandas E, Goncalves LG, Belinha A, Cunha C, Oosting M, Joosten LAB, Matarese G, van Crevel R, Netea MG. Immunometabolic Pathways in BCG-Induced Trained Immunity. Cell Rep. 2016; 17:2562–2571. [PubMed: 27926861]

47. Zhao Q, Chu Z, Zhu L, Yang T, Wang P, Liu F, Huang Y, Zhang F, Zhang X, Ding W, Zhao Y. 2-Deoxy-d-Glucose Treatment Decreases Anti-inflammatory M2 Macrophage Polarization in Mice with Tumor and Allergic Airway Inflammation. Front Immunol. 2017; 8:637. [PubMed: 28620389]

48. Serhan CN, Brain SD, Buckley CD, Gilroy DW, Haslett C, O'Neill LA, Perretti M, Rossi AG, Wallace JL. Resolution of inflammation: state of the art, definitions and terms. FASEB J. 2007; 21:325–332. [PubMed: 17267386]

49. Fei F, Lee KM, McCarry BE, Bowdish DM. Age-associated metabolic dysregulation in bone marrow-derived macrophages stimulated with lipopolysaccharide. Sci Rep. 2016; 6:22637. [PubMed: 26940652]

50. Cuesta N, Salkowski CA, Thomas KE, Vogel SN. Regulation of lipopolysaccharide sensitivity by IFN regulatory factor-2. J Immunol. 2003; 170:5739–5747. [PubMed: 12759457]

51. Salkowski CA, Kopydlowski K, Blanco J, Cody MJ, McNally R, Vogel SN. IL-12 is dysregulated in macrophages from IRF-1 and IRF-2 knockout mice. J Immunol. 1999; 163:1529–1536. [PubMed: 10415056]

52. Salkowski CA, Barber SA, Detore GR, Vogel SN. Differential dysregulation of nitric oxide production in macrophages with targeted disruptions in IFN regulatory factor-1 and -2 genes. J Immunol. 1996; 156:3107–3110. [PubMed: 8617930]

53. Harada H, Fujita T, Miyamoto M, Kimura Y, Maruyama M, Furia A, Miyata T, Taniguchi T. Structurally similar but functionally distinct factors, IRF-1 and IRF-2, bind to the same regulatory elements of IFN and IFN-inducible genes. Cell. 1989; 58:729–739. [PubMed: 2475256]

54. Hida S, Ogasawara K, Sato K, Abe M, Takayanagi H, Yokochi T, Sato T, Hirose S, Shirai T, Taki S, Taniguchi T. CD8(+) T cell-mediated skin disease in mice lacking IRF-2, the transcriptional attenuator of interferon-alpha/beta signaling. Immunity. 2000; 13:643–655. [PubMed: 11114377]

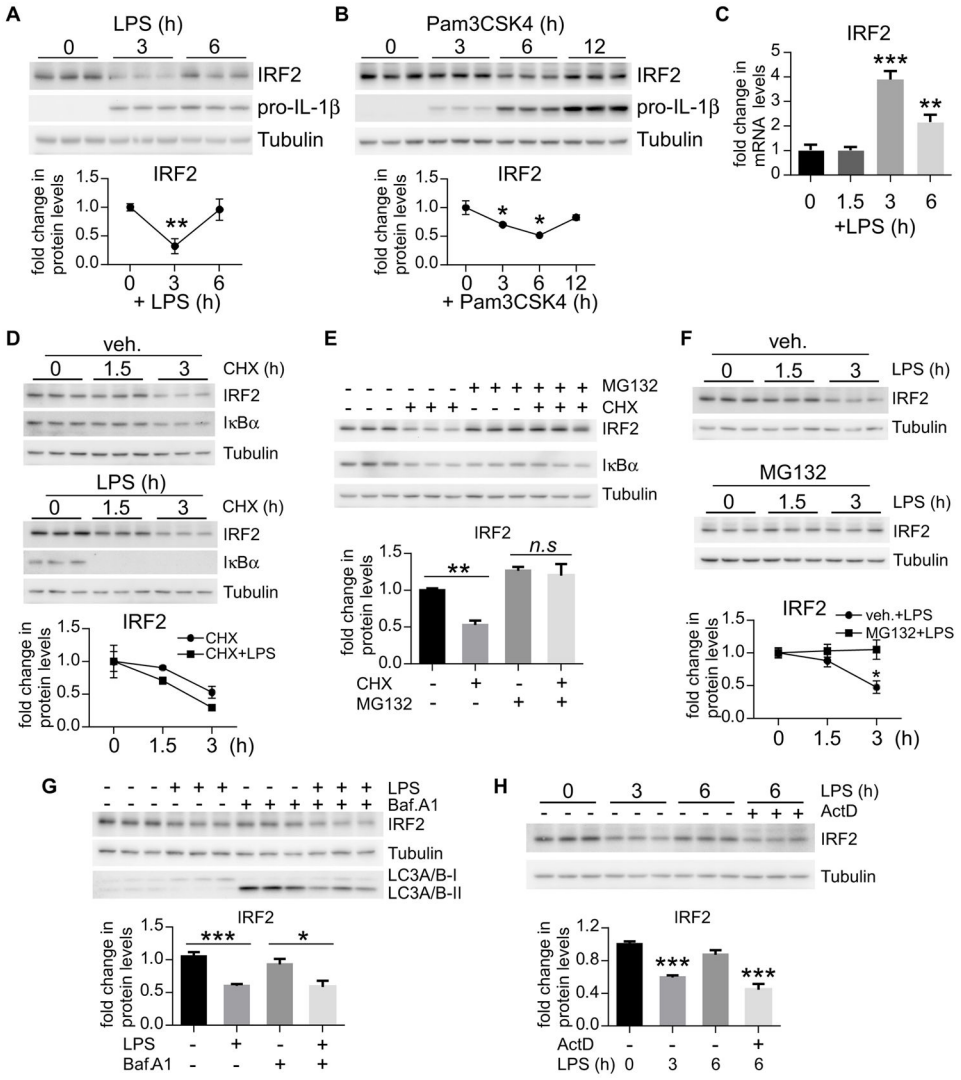

Figure 1. IRF2 undergoes early degradation in response to LPS stimulation in macrophages

(A–C) BMDMs were treated with 100 ng/ml LPS (A and C) or 1 μg/ml Pam3CSK4 (B) for the indicated duration of time. Levels of IRF2 and pro-IL-1β were determined by Western blotting and densitometric analyses performed using ImageJ (NIH) (A–B); mRNA levels of IRF2 were determined by real-time PCR (C). A–B, n=3; mean±SD; * p<0.05, ** p<0.01 compared to untreated control group; C, n=4; mean±SD; ** p<0.01, *** p<0.001 compared to untreated control group. (D) BMDMs were treated with or without 5 μg/ml cycloheximide (CHX) or CHX plus 100 ng/ml LPS for 1.5 and 3 h. Levels of IRF2 and IκBα were determined by Western blotting and densitometric analyses performed. (E) BMDMs were pre-treated with or without 10 μM MG132 for 30 min, followed by treatment with or without 5 μg/ml CHX for another 3 h. Levels of IRF2 and IκBα were determined by Western blotting and densitometric analyses performed. n=3; mean±SD; ** p<0.01 compared to untreated control group. (F) BMDMs were pre-treated with or without 10 μM MG132 for 30 min, followed by treatment with or without 100 ng/ml LPS for 1.5 and 3 h. Levels of IRF2 were determined by Western blotting and densitometric analyses performed. n=3; mean±SD;

* $p<0.05$ compared to untreated control group. (G) BMDMs were pre-treated with or without 10 nM Bafilomycin A1 (Baf.A1) for 30 min, followed by treatment with or without 100 ng/ml LPS for another 3 h. Levels of IRF2 were determined by Western blotting and densitometric analyses performed. n=3; mean±SD; *** $p<0.001$ compared to untreated control group; * $p<0.05$, compared to Balf.A1 treated, LPS untreated group. (H) BMDMs were treated with or without 100 ng/ml LPS or LPS plus 1 μg/ml actinomycin D (ActD) for 3 and 6 h. Levels of IRF2 were determined by Western blotting and densitometric analyses performed. n=3; mean±SD; *** $p<0.001$ compared to untreated control group.

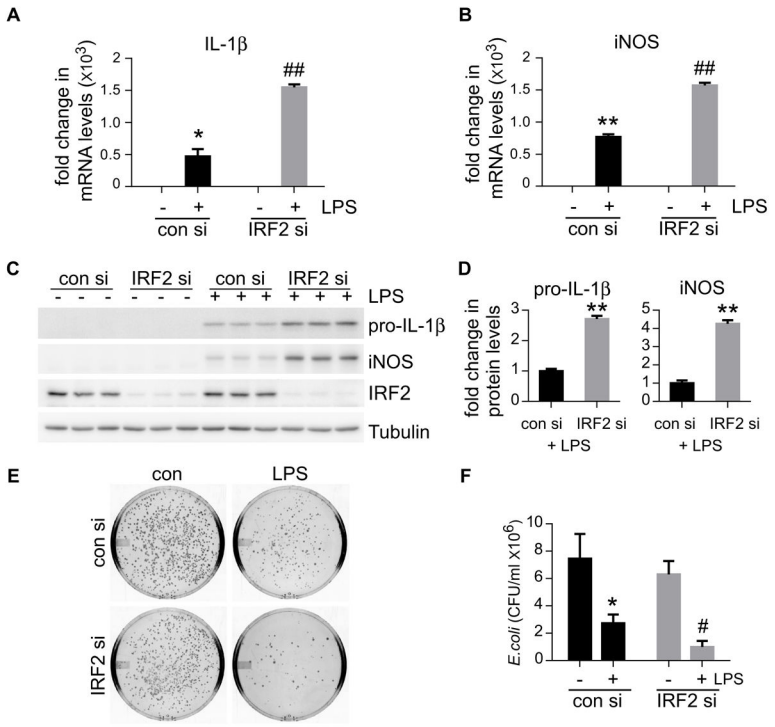

Figure 2. IRF2 knockdown promotes inflammatory response in LPS treated macrophages

(A–B) BMDMs were transfected with 20 nM control siRNAs or IRF2 siRNAs. Forty-eight hours after transfection, cells were treated with 100 ng/ml LPS for 4 h. mRNA levels of IL-1β (A) and iNOS (B) were determined by real-time PCR. n=3; mean±SD; * $p<0.05$, ** $p<0.01$ compared to untreated control siRNA (con si) group; ## $p<0.01$ compared to LPS treated con si group. (C–D) BMDMs were transfected with control siRNAs or IRF2 siRNAs. Forty-eight hours after transfection, cells were treated with 100 ng/ml LPS for 6 h. Levels of pro- IL-1β, iNOS and IRF2 were determined by Western blotting and densitometric analyses performed using ImageJ. n=3; mean±SD; ** $p<0.01$ compared to LPS treated con si group. (E–F) BMDMs were transfected and treated with LPS as in C–D. After LPS treatment, live E. coli were added into the media. One hour after incubation, the supernatants were collected and cultured on Luria broth agar plates at 37 °C for 24 h. The bacteria colonies were counted and the cfu of E. coli in the supernatants were determined. n=3; mean±SD; * $p<0.05$ compared to untreated con si group; # $p<0.05$ compared to LPS treated con si group.

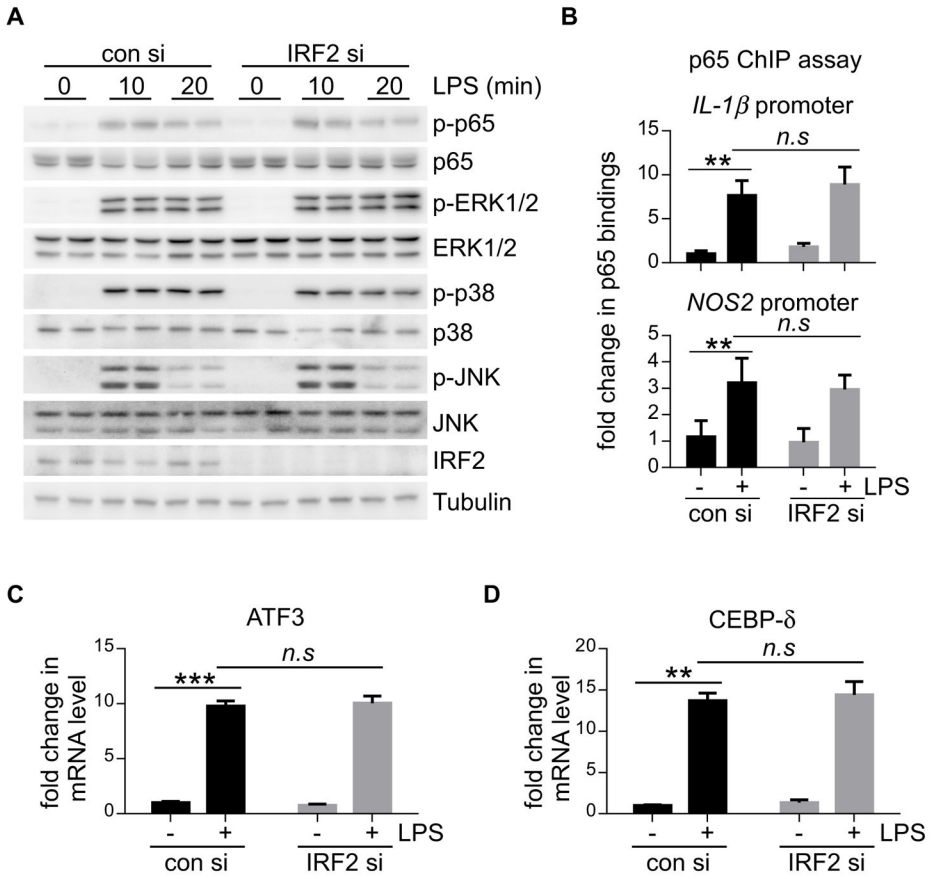

Figure 3. IRF2 knockdown has no effects on proximal signaling events upon LPS stimulation or the expression of several key regulators of LPS induced inflammation in macrophages

(A) BMDMs were transfected with 20 nM control siRNAs or IRF2 siRNAs. Forty-eight hours after transfection, cells were treated with 100 ng/ml LPS for 10 and 20 min. Levels of the indicated proteins were determined by Western blotting. (B) BMDMs were transfected with control siRNAs or IRF2 siRNAs. Forty-eight hours after transfection, cells were treated with 100 ng/ml LPS for another 1 h. Cells were collected and bindings of p65 to *IL-1β* and *NOS2* promoters were determined by ChIP assay. n=4; mean±SD; ** $p<0.01$ compared to untreated con si group. (C–D) BMDMs were transfected with control siRNAs or IRF2 siRNAs. Forty-eight hours after transfection, cells were treated with 100 ng/ml LPS for 4 h. mRNA levels of ATF3 and CEBP-δ were determined by real-time PCR. n=3; mean±SD; ** $p<0.01$, *** $p<0.001$ compared to untreated con si group.

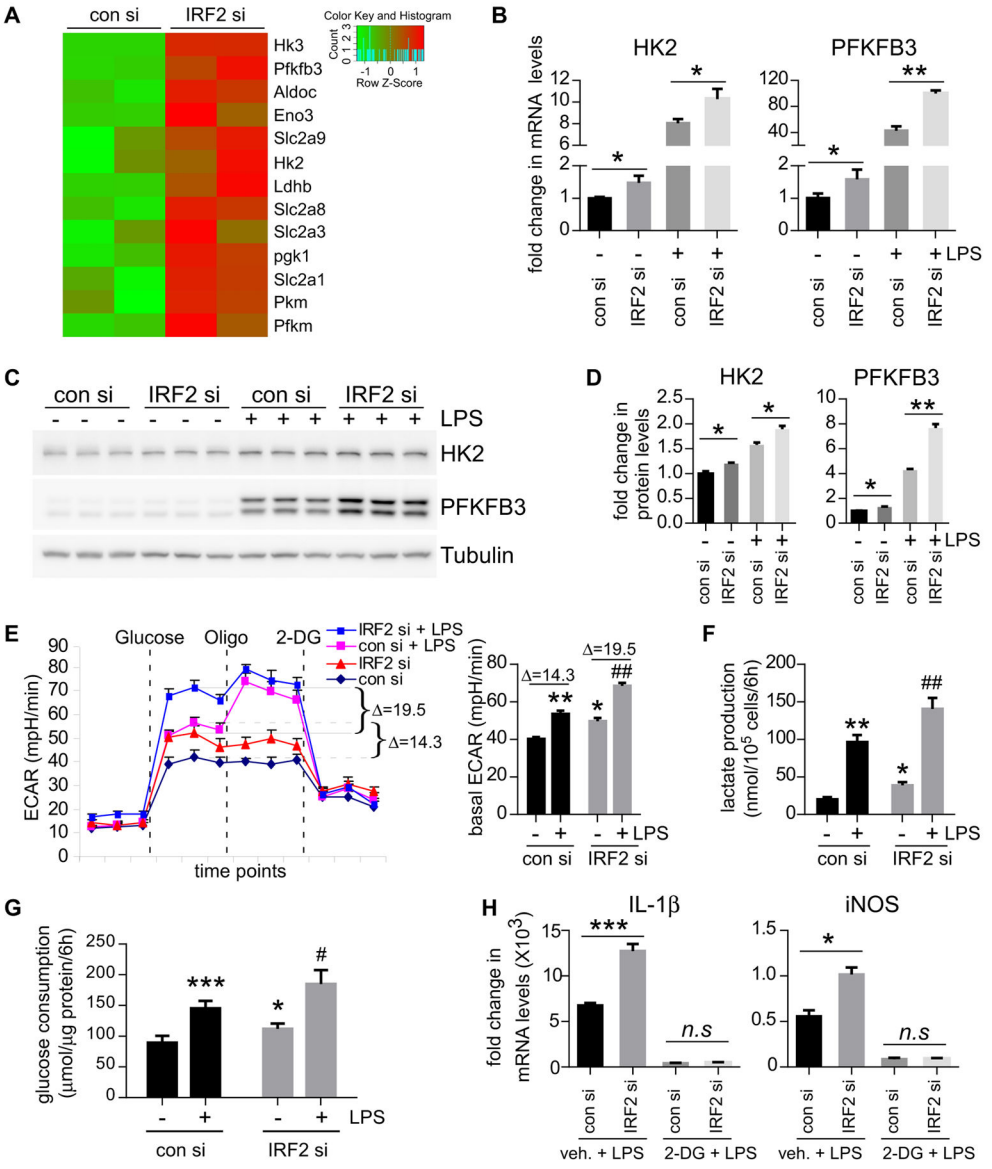

Figure 4. IRF2 knockdown promotes glycolysis in macrophages

(A) BMDMs were transfected with 20 nM control siRNAs or IRF2 siRNAs. Forty-eight hours after transfection, the cells were collected, total RNAs purified and RNA sequencing performed. Heatmap of differentially expressed key glycolytically associated genes between two groups is presented, with average expression levels indicated by color scale from green (low expression) to red (high expression). (B) BMDMs were transfected as in A. Forty-eight hours after transfection, cells were treated with or without 100 ng/ml LPS for 4 h. mRNA levels of HK2 and PFKFB3 were determined by real-time PCR. n=4; mean±SD; * p<0.05, ** p<0.01 compared to respective con si group. (C–D) BMDMs were transfeted as in A and B. Forty-eight hours after transfection, cells were treated with 100 ng/ml LPS for 6 h. Levels of HK2 and PFKFB3 were determined by Western blotting and densitometric analyses performed using ImageJ. n=3; mean±SD; * p<0.05, ** p<0.01 compared to respective con si group. (E) BMDMs were seeded in Seahorse XF-24 cell culture microplates and transfected

with 20 nM control siRNAs or IRF2 siRNAs. Forty-eight hours after transfection, cells were treated with or without 100 ng/ml LPS for 6 h, followed by sequential treatment with glucose, oligomycin (oligo) and 2-DG. Real-time extracellular acidification rate (ECAR) was recorded and basal ECAR values plotted. n=5,6,5,6; mean±SEM; * $p<0.05$, ** $p<0.01$ compared to untreated con si group; ## $p<0.01$ compared to LPS treated con si group. (F–G) BMDMs were transfected with control siRNAs or IRF2 siRNAs. Forty-eight hours after transfection, cells were washed twice and treated with or without 100 ng/ml LPS for 6 h. Supernatants were collected and levels of lactate and glucose measured respectively. F, n=3; G, n=5; mean±SD; * $p<0.05$, ** $p<0.01$, *** $p<0.001$ compared to untreated con si group; # $p<0.05$, ## $p<0.01$ compared to LPS treated con si group. (H) BMDMs were transfected with con siRNAs or IRF2 siRNAs. Forty-eight hours after transfection, cells were pre-treated with or without 10 mM 2-DG for 1 h, followed by 100 ng/ml LPS treatment for an additional 4 h. mRNA levels or IL-1β and iNOS were determined by real-time PCR. n=4; mean±SD; * $p<0.05$, *** $p<0.001$ compared to vehicle plus LPS treated control group.

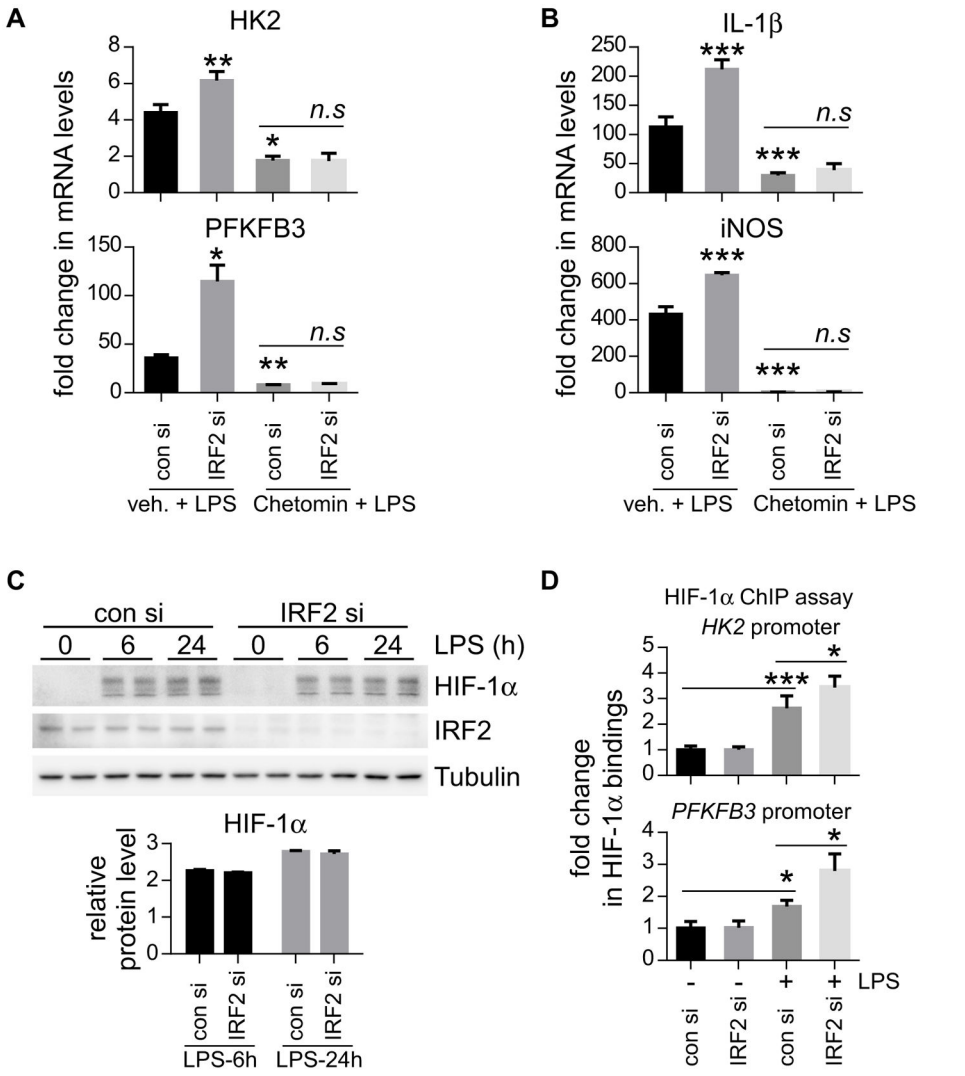

Figure 5. IRF2 regulated glycolysis and inflammation are dependent on HIF-1α in macrophages

(A) BMDMs were transfected with 20nM control siRNAs or IRF2 siRNAs. Forty-eight hours after transfection, cells were pre-treated with or without 100 nM Chetomin for 1 h, followed by LPS treatment (100 ng/ml) for an additional 4 h. mRNA levels or HK2 and PFKFB3 were determined by real-time PCR. n=3; mean±SD; * p<0.05, ** p<0.01 compared to vehicle plus LPS treated con si group. (B) BMDMs were transfected and treated as in A. mRNA levels or IL-1β and iNOS were determined by real-time PCR. n=3; mean±SD; *** p<0.01 compared to vehicle plus LPS treated con si group. (C) BMDMs were transfected with control siRNAs or IRF2 siRNAs. Forty-eight hours after transfection, cells were treated with 100 ng/ml LPS for 6 and 24 h. Protein levels of HIF-1α and IRF2 were determined by Western blotting. Densitometric analyses of HIF-1α levels were performed using ImageJ. (D) Macrophages were transfected with control siRNAs or IRF2 siRNAs. Forty-eight hours after transfection, cells were treated with or without 100 ng/ml LPS for 4 h. Cells were collected and bindings of HIF-1α to the *HK2* and *PFKFB3* promoters were determined by ChIP assay. n=4; mean±SD; * p<0.05, ** p<0.01 compared to respective control group.

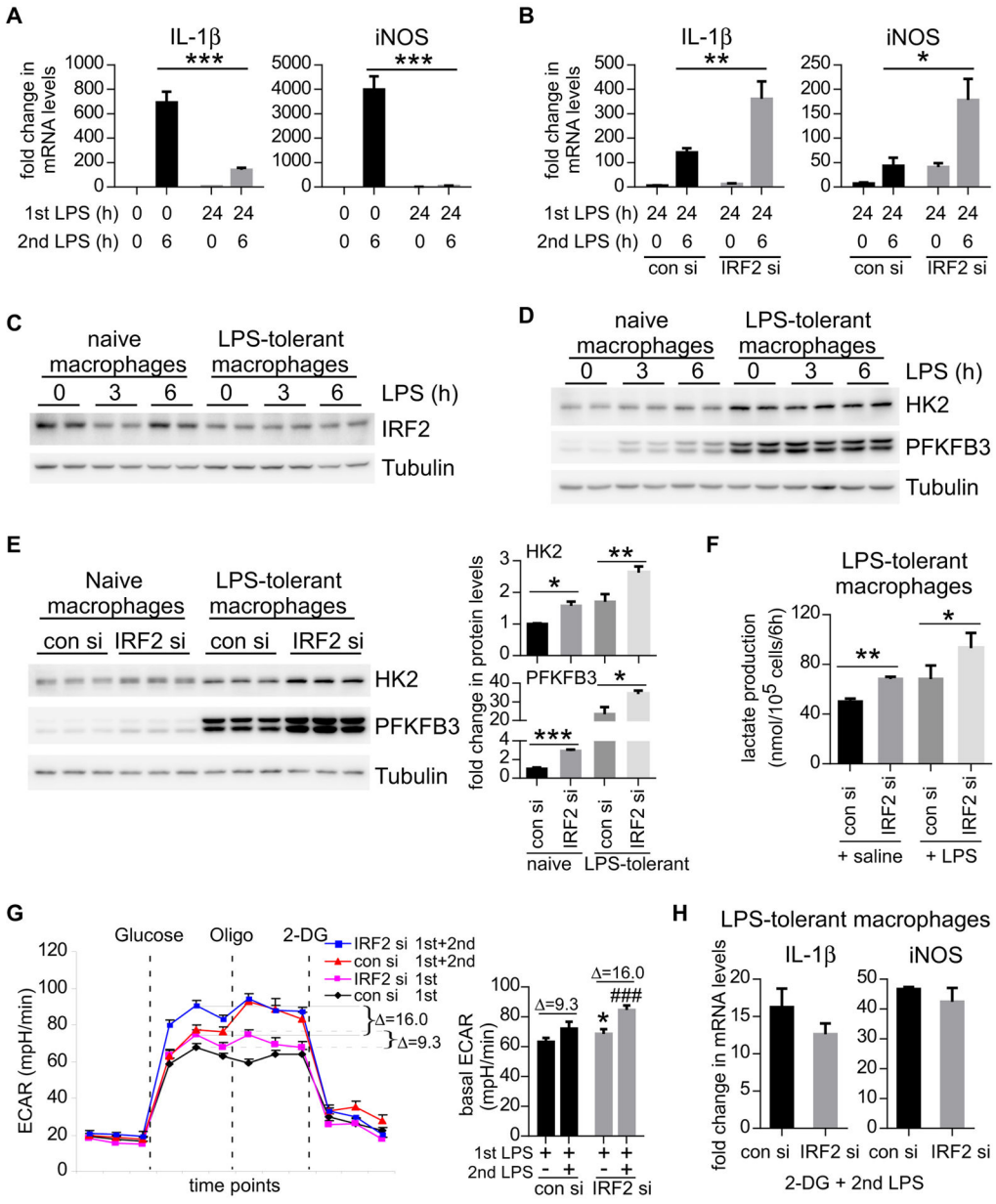

Figure 6. IRF2 knockdown relieves endotoxin tolerance in macrophages

(A) BMDMs were treated with or without 100 ng/ml LPS for 24 h. Cells were washed twice and re-treated with LPS for 4 h. mRNA levels of IL-1β and iNOS were determined by real-time PCR. n=4; mean±SD; *** p<0.001. (B) BMDMs were transfected with control siRNAs or IRF2 siRNAs. Twenty-four hours after transfection, cells were treated with 100 ng/ml LPS for 24 h. Cells were then washed twice and re-treated with or without 100 ng/ml LPS for an additional 4 h. mRNA levels of IL-1β and iNOS were determined by real-time PCR. n=4; mean±SD; * p<0.05, ** p<0.01. (C–D) BMDMs were treated with or without 100 ng/ml LPS for 24 h. Cells were washed twice and re-treated with LPS for 3 and 6 h. Levels of IRF2 (C), HK2 (D) and PFKFB3 (D) were determined by Western blotting. (E) BMDMs were transfected with control siRNAs or IRF2 siRNAs followed by treatment with or

without LPS (100 ng/ml) for 24 h. Cells were washed twice and cultured in fresh media for another 6 h. Levels of HK2 and PFKFB3 were determined by Western blotting and densitometric analyses performed using ImageJ. n=3; mean±SD; * $p<0.05$, ** $p<0.01$, *** $p<0.001$ compared to respective control group. (F) BMDMs were transfected with control siRNAs or IRF2 siRNAs and treated with LPS (100 ng/ml) for 24 h. Cells were washed twice and re-treated with or without LPS (100ng/ml) for another 6 h. Media were collected and lactate levels in the media were determined by lactate assay kit. n=4; mean±SD; * $p<0.05$, ** $p<0.01$ compared to respective con si group. (G) BMDMs were seeded in Seahorse XF-24 cell culture microplates and transfected with 20 nM control siRNAs or IRF2 siRNAs. Twenty-four hours after transfection, cells were treated with 100 ng/ml LPS for 24 h. The cells were washed twice and re-treated with or without 100 ng/ml LPS for another 6 h, followed by sequential treatment with glucose, oligomycin (oligo) and 2-DG. Real-time ECAR was recorded and basal ECAR values plotted. n=5,6,5,6; mean±SEM; * $p<0.05$ compared to 2^{nd} LPS untreated con si group; ### $p<0.001$ compared to 2^{nd} LPS treated con si group. (H) BMDMs were transfected with control siRNAs or IRF2 siRNAs and treated with LPS (100 ng/ml) for 24 h. Cells were washed twice and pre-treated with 10 mM 2-DG for 1 h, followed by treatment with or without LPS (100 ng/ml) for another 4h. mRNA levels of IL-1β and iNOS were determined by real-time PCR. n=3; mean±SD.

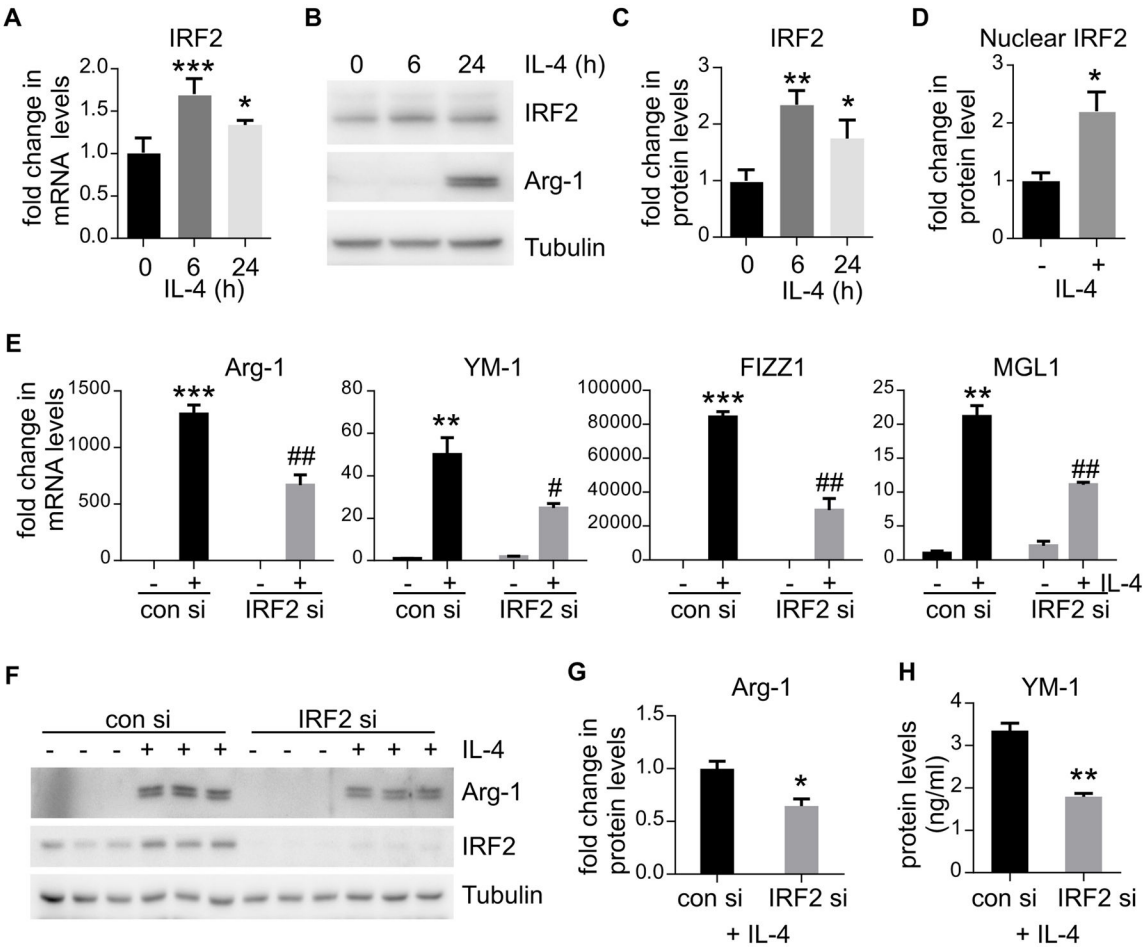

Figure 7. IRF2 participates in alternative activation of macrophages by IL-4

(A–C) BMDMs were treated with 5 ng/ml IL-4 for 6 and 24 h. mRNA levels of IRF2 were determined by real-time PCR (A); protein levels of IRF2 and Arg-1 were determined by Western blotting and densitometric analyses performed using ImageJ (B–C). n=3; mean ±SD; * p<0.05, ** p<0.01, *** p<0.001 compared to untreated control group. (D) BMDMs were treated with or without 5ng/ml IL-4 for 6 h. Cells were collected and nuclear fractions isolated. Protein levels of IRF2 in the nuclei were determined by Western blotting and densitometric analyses performed using ImageJ. n=3; mean±SD; * p<0.05 compared to untreated control group. (E) BMDMs were transfected with 20 nM control siRNAs or IRF2 siRNAs. Tenty-four after transfection, cells were treated with or without 5 ng/ml IL-4 for 24 h. mRNA levels of Arg-1, YM-1, FIZZ1 and MGL1 were determined by real-time PCR. n=3; mean±SD; ** p<0.01, *** p<0.001 compared to untreated con si group; # p<0.05, ## p<0.01 compared to IL-4 treated con si group. (F–H) BMDMs were transfected with control siRNAs or IRF2 siRNAs and treated with IL-4 as in E. Cellular levels of Arg-1 and IRF2 were determined by Western blotting (F) and densitometric analyses performed using ImageJ (G). Secreted YM-1 levels in the media were determined by ELISA assay (H). n=3; mean±SD; * p<0.05, ** p<0.01 compared to IL-4 treated con si group.

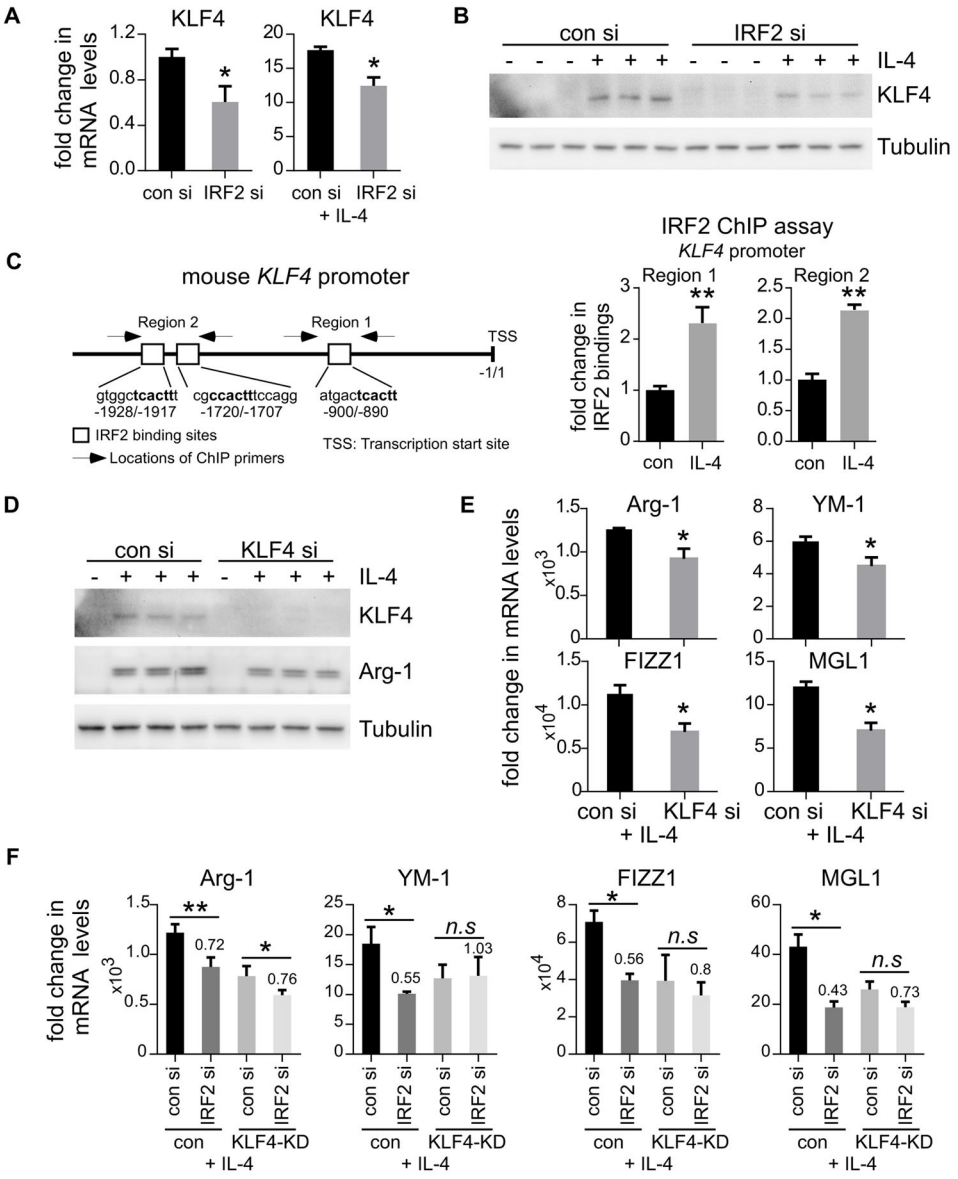

Figure 8. IRF2 promotion of alternative activation of macrophages by IL-4 is KLF4-dependent

(A–B) BMDMs were transfected with 20 nM control siRNAs or IRF2 siRNAs. Twenty-four hours after transfection, cells were treated with or without 5 ng/ml IL-4 for another 24 h. Levels of KLF4 were determined by real-time PCR (A) and Western blotting (B). A, n=4; mean±SD; * p<0.05 compared to respective con si group. (C) BMDMs were treated with 5 ng/ml IL-4 for 6 h. Cells were collected and bindings of IRF2 to the *KLF4* promoter determined by ChIP assay. A schematic diagram of the *KLF4* promoter region containing the putative IRF2 binding elements (in bold) is shown. n=4; mean±SD; ** p<0.01 compared to untreated control group. (D) BMDMs were transfected with control siRNAs or KLF4 siRNAs. Twenty-four hours after transfection, cells were treated with or without 5 ng/ml IL-4 for 24 h. Levels of KLF4 and Arg-1 were determined by Western blotting. (E) BMDMs were transfected and treated as in D. mRNA levels of Arg-1, YM-1, FIZZ1 and MGL1 were determined by real-time PCR. n=3; mean±SD; * p<0.05 compared to IL-4 treated con si

group. (F) BMDMs were transfected with 20 nM control siRNAs or KLF4 siRNAs. Twenty-four hours after transfection, cells were re-transfected with control siRNAs or IRF2 siRNAs. Twenty-four hours after the 2nd transfection, cells were treated with or without IL-4 (5 ng/ml) for another 24 h. mRNA levels of Arg-1, YM-1, FIZZ1 and MGL1 were determined by real-time PCR. n=3; mean±SD; * $p<0.05$, ** $p<0.01$ compared to respective control group.